

Supplementary Information

Sublimable cationic iridium(III) complexes for red-emitting diodes with high colour purity

Ruihuan Liu^a, Dongxin Ma^{*a}, Lian Duan^{*ab}

^aKey Lab of Organic Optoelectronics & Molecular Engineering of Ministry of Education, Department of Chemistry, Tsinghua University, Beijing 100084, P. R. China

^bCenter for Flexible Electronics Technology, Tsinghua University, Beijing 100084, P. R. China

E-mail: duanl@mail.tsinghua.edu.cn, madongxin@tsinghua.edu.cn

Supplemental Experimental Section

- 1. Experimental Procedures**
- 2. Supporting Figures**
- 3. Supporting Tables**

1. Experimental Procedures

Structural Characterization Methods. ^1H -NMR and ^{19}F -NMR spectra were recorded on a JOEL JNM-ECA600 NMR spectrometer. ESI mass spectrometry was performed with Thermo Electron Corporation Finnigan LTQ.

X-Ray Crystallography. The single crystal X-ray diffraction data collections were carried out on a Rigaku AFC-10/Saturn 724+ charge-coupled device (CCD) diffractometer equipped with graphite-monochromatized Mo K α radiation ($\lambda = 0.71073 \text{ \AA}$) using the multi-scan technique. The structures were determined by direct methods using SHELXS-97 and refined by full-matrix least-squares procedures on F2 with SHELXL-2008. All the non-hydrogen atoms were obtained from the difference Fourier map and subjected to anisotropic refinement by full-matrix least squares on F2. The hydrogen atoms were obtained geometrically and treated as riding on the parent atoms or constrained in the locations during refinements.

Photophysical, Electrochemical and Thermal Measurements. Absorption and photoluminescence (PL) spectra were characterized with an ultraviolet-visible spectrophotometer (Agilent 8453) and a fluorospectrophotometer (HITACHI, F-7000), respectively. Photoluminescence quantum yields (PLQYs) in degassed anhydrous acetonitrile solutions and neat film were measured at the excitation wavelength of 400 nm (Hamamatsu Photonics K. K., C9920-03). The excited state lifetimes were measured by a lifetime and steady state spectrometer (Edinburgh Instruments, FLS 980) with time-correlated single-photon counting technique at the peak emitting wavelength. Cyclic voltammetry was proved in oxygen-free anhydrous solutions on a Princeton Applied Research potentiostat/ galvanostat

Model 283 voltammetric analyzer at a scan rate of 100 mV s^{-1} with a platinum plate as the working electrode, a silver wire as the pseudo-reference electrode and a platinum wire as the counter electrode. Oxidation potentials were measured in *N,N*-dimethyl formamide with tetrabutylammonium perchlorate (40 mg mL^{-1}) as the supporting electrolyte, while reduction potentials were performed in acetonitrile with tetrabutylammonium hexafluorophosphate (35 mg mL^{-1}) as the supporting electrolyte. Ferrocene served as the internal standard. Thermal stability was measured by a thermogravimetric analyzer (TA Instruments Q5000) with a heating rate of $10^\circ\text{C min}^{-1}$ under nitrogen flows.

Quantum Chemical Calculations. Calculations on the volume of both the coordinated iridium (III) cations and tetraphenylborate-type anions were performed by means of DFT using ‘opt=tight rb3lyp/gen geom=connectivity pseudo=read’. Calculations on the ground electronic states of the emissive coordinated iridium (III) cations were performed by means of DFT using ‘opt=tight rb3lyp/gen geom=connectivity pseudo=read’. Calculations on the excited electronic states of the emissive coordinated iridium (III) cations were performed by means of TD-DFT using ‘td=(50-50,nstates=5) b3lyp/gen geom=connectivity pseudo=read’. The double- ξ quality basis sets were 6-31G* for the carbon, hydrogen, nitrogen, fluorine and LANL2DZ for iridium. The inner core electrons of iridium (III) were replaced by an effective core potential (ECP), with outer core of $5s^2 5p^6$ electrons and the $5d^6$ valence electrons. All the quantum chemical calculations were performed with Gaussian 09 software package using a spin restricted formalism (see the reference).

Device fabrication and evaluation. OLEDs were grown on cleaned, ultraviolet-ozone-treated and indium-tin-oxide-coated glass substrates, with a sheet resistance of about 20Ω per sq. Each functional layer was fabricated thereon successively by vacuum evaporation deposition under a low pressure below 5×10^{-4} Pa. Each device shows an active area of $3.0 \times 3.0 \text{ mm}^2$. Current density-luminance-voltage (*J-L-V*) characteristics were collected with Keithley 4200 semiconductor system, while electroluminescence (EL) spectra were recorded by a Photo Research PR705 spectrophotometer. Device measurements were carried out at room temperature in the ambient air without further encapsulation.

2. Supporting Figures

Scheme S1. Synthetic routes of complexes **1** and **2**.

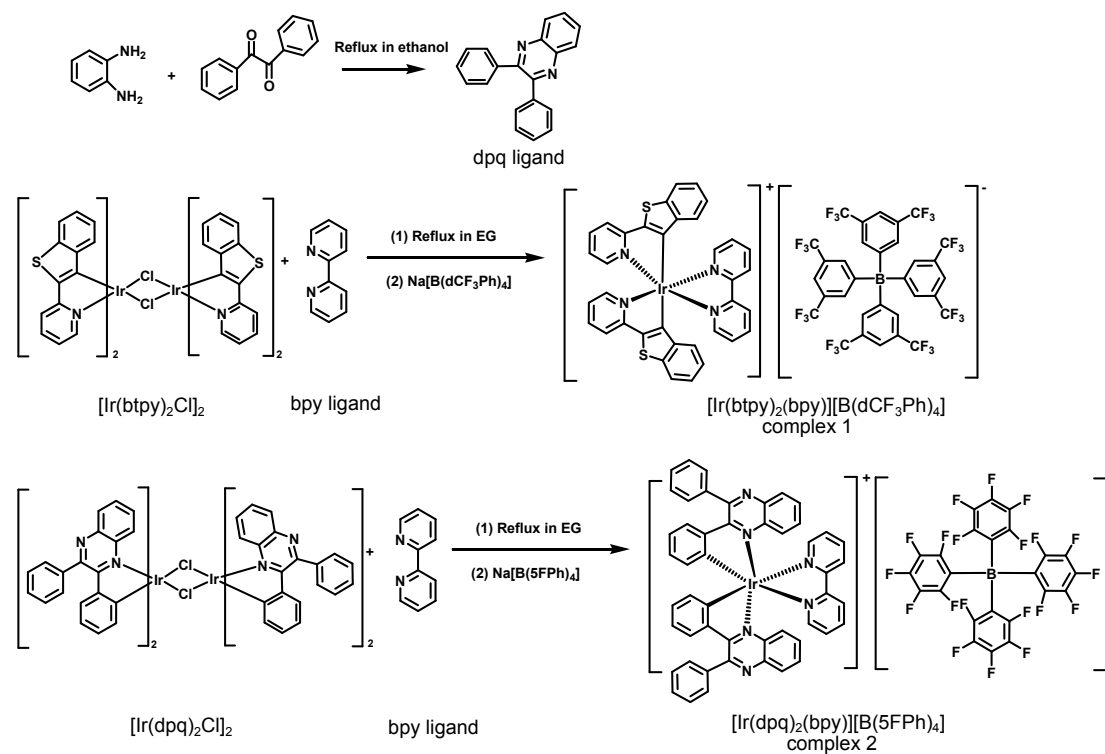


Fig. S1. The single-crystal structure of $[\text{Ir}(\text{btpy})_2(\text{bpy})][\text{B}(\text{dCF}_3\text{Ph})_4]$ (complex **1**). Here the thermal ellipsoids are drawn at the 30% probability level. The solvent molecules and hydrogen atoms are omitted for clarity. The unlabeled atoms are carbon atoms.

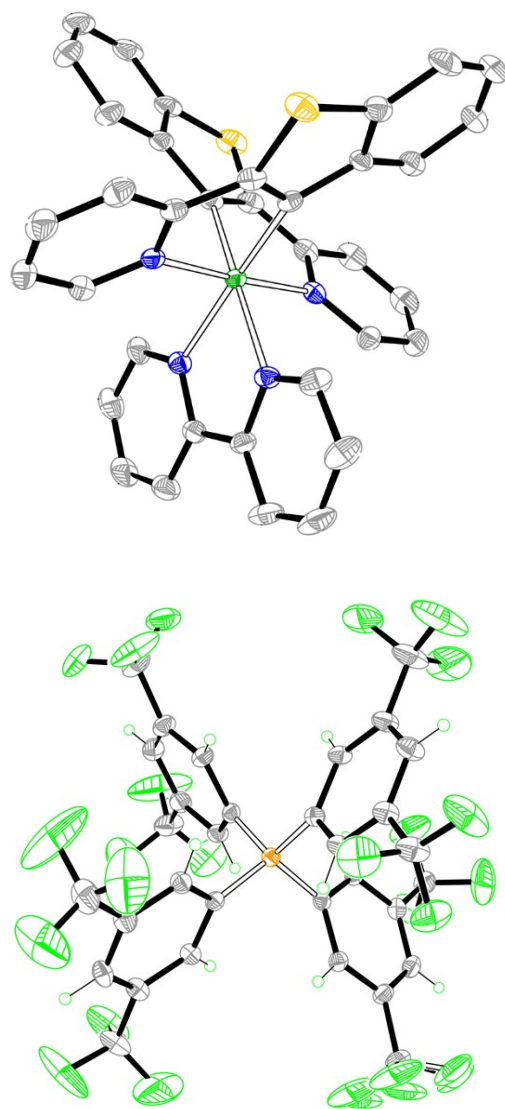


Fig. S2. (a) Absorption spectra and (b) the excited state lifetime in neat films at 298 K of complexes **1** and **2**.

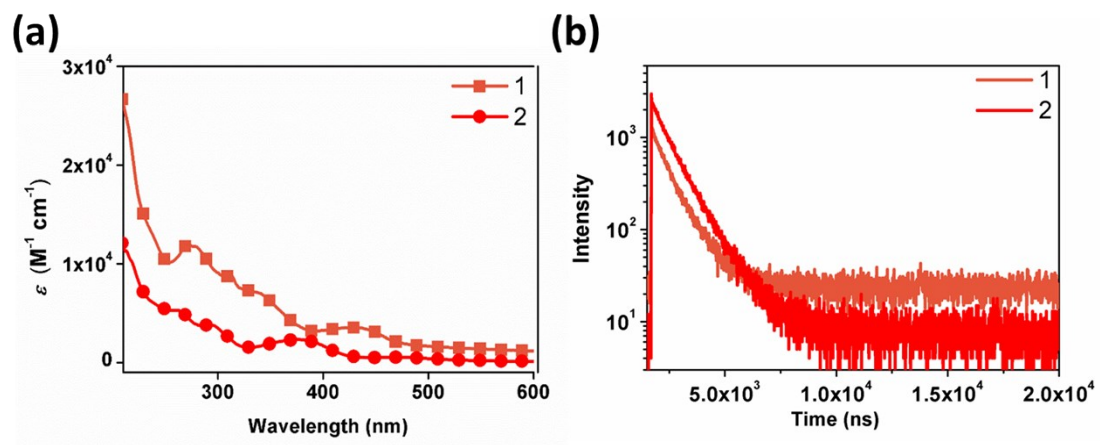


Fig. S3. Cyclic voltammogram of complexes 1 and 2 in oxygen-free anhydrous solutions with potentials recorded versus the ferrocenium/ ferrocene (Fc^+ / Fc) couple.

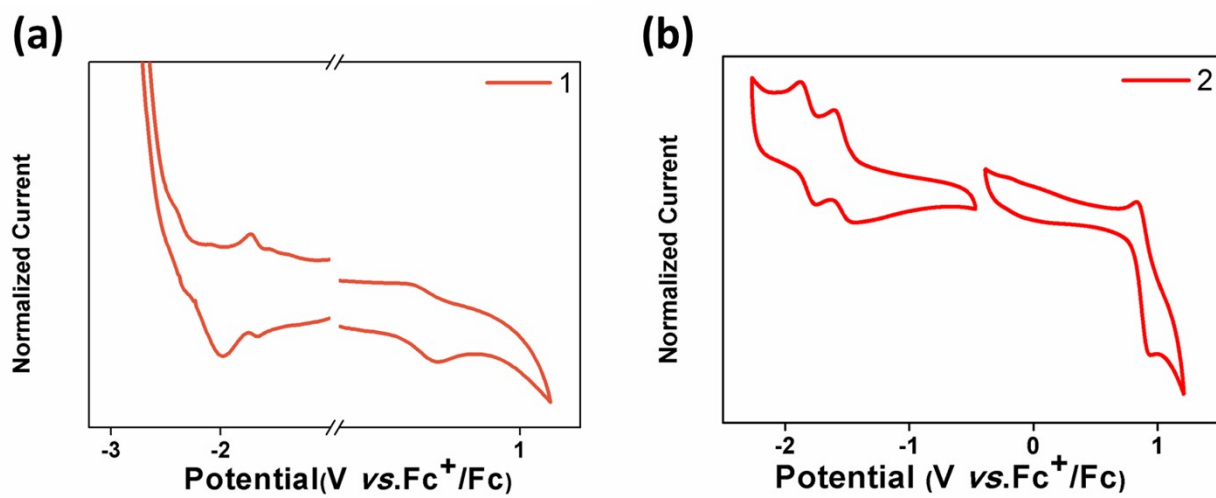


Fig. S4. TGA of complexes **1** and **2** under nitrogen-flow conditions.

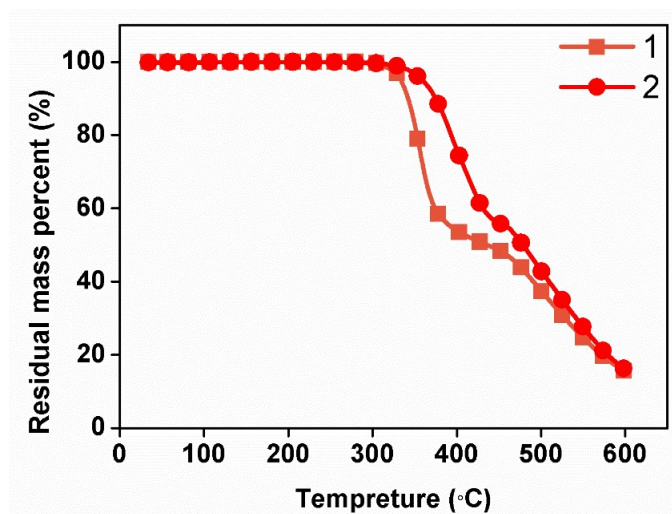


Fig. S5. MO surfaces of complex 1 ($|\Psi| = 0.02$).

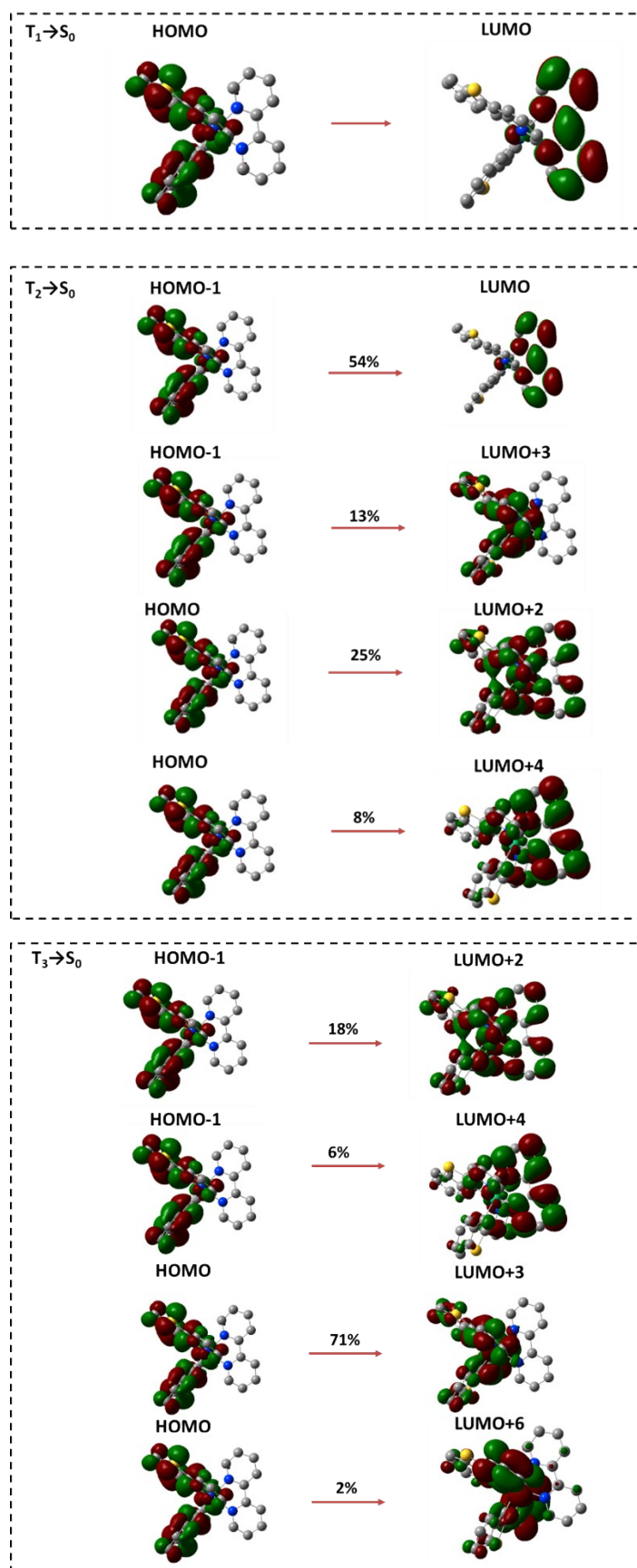


Fig. S6. MO surfaces of complex **2** ($|\Psi| = 0.02$).

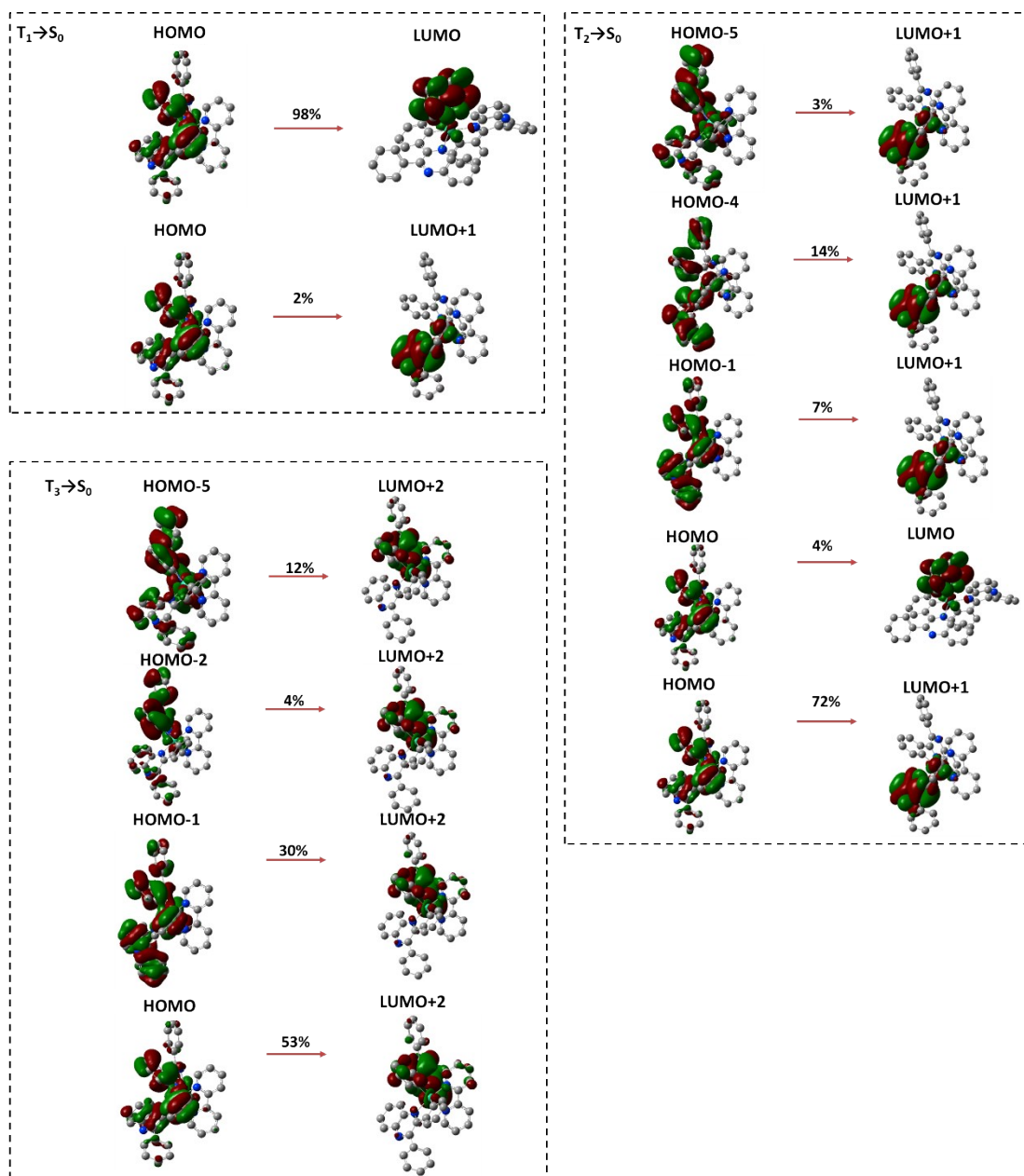


Fig. S7. Characteristics of OLEDs based on complex **1** with the structure of ITO/ HATCN (5 nm)/ NPB (40 nm)/ TCTA (10 nm)/ DIC-TRZ: $x\%$ complex **1** (12 nm)/ BPBiPA (50 nm)/ LiF (1 nm)/ Al (150 nm) at varying dopant concentrations. (a) Current density-voltage, (b) Luminance-voltage, (c) Current efficiency-luminance curves, (d) EL spectra.

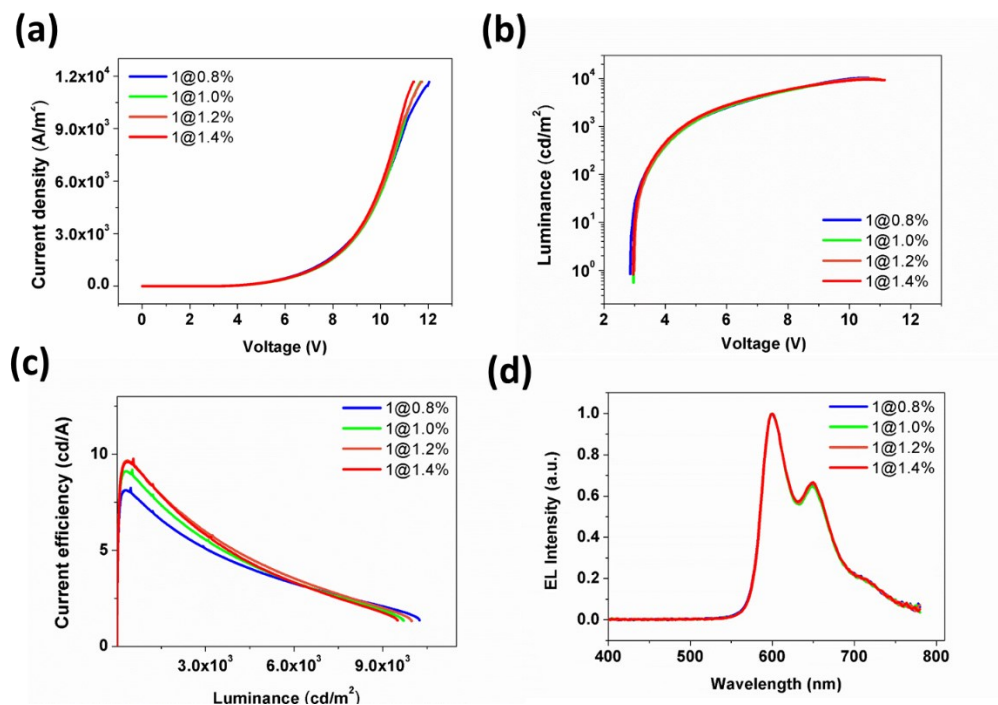
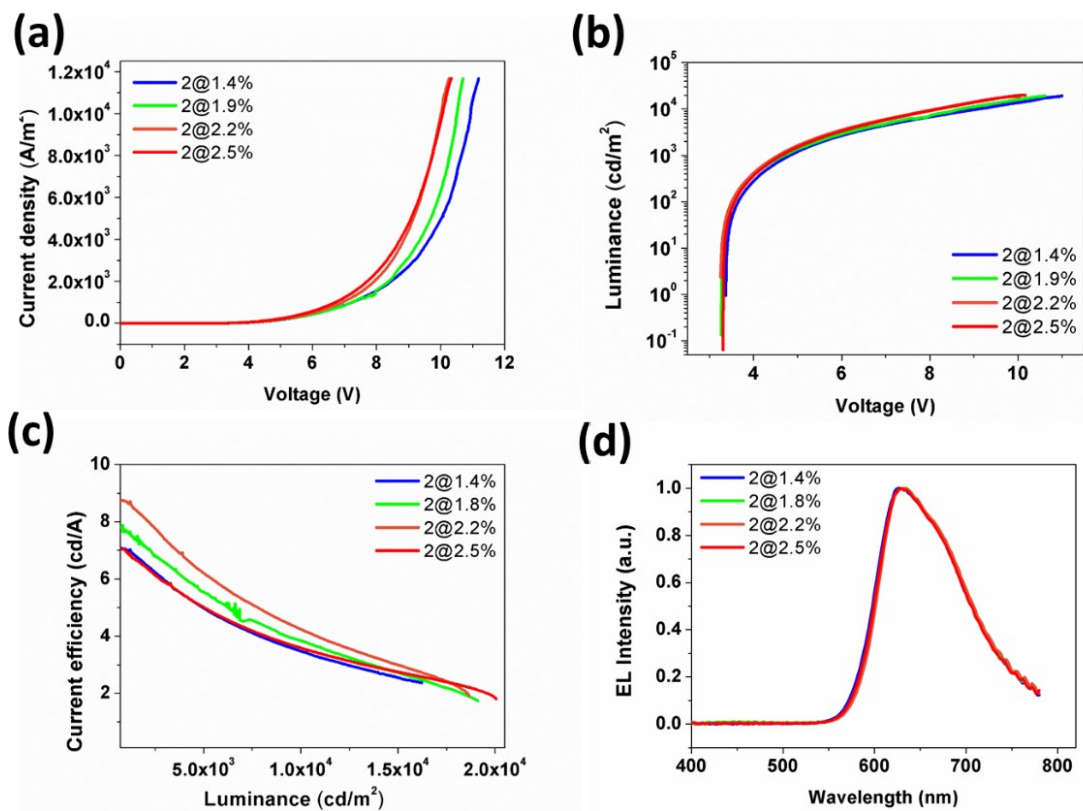


Fig. S8. Characteristics of OLEDs based on complex **2** with the structure of ITO/ HATCN (5 nm)/ NPB (40 nm)/ TCTA (10 nm)/ DIC-TRZ: $x\%$ complex **2** (12 nm)/ BPBiPA (50 nm)/ LiF (1 nm)/ Al (150 nm) at varying dopant concentrations. (a) Current density-voltage, (b) Luminance-voltage, (c) Current efficiency-luminance curves, (d) EL spectra.



3. Supporting Tables

Table S1. Bond lengths and angles of complex **1** from X-ray crystallography data.

	Ir-C (Å)	Ir-N (Å)	Angles(°)
Molecule 1	Ir(1)-C(20) 2.014	Ir(1)-N(1) 2.062	C(20)-Ir(1)-N(2) 79.87
		Ir(1)-N(2) 2.067	C(7)-Ir(1)-N(1) 79.69
	Ir(1)-C(7) 2.009	Ir(1)-N(3) 2.119	N(3)-Ir(1)-N(4) 76.61
		Ir(1)-N(4) 2.143	
Molecule 2	Ir(2)-C(47) 2.018	Ir(2)-N(5) 2.058	C(47)-Ir(2)-N(5) 79.51
		Ir(2)-N(6) 2.063	C(60)-Ir(2)-N(6) 79.89
	Ir(2)-C(60) 2.046	Ir(2)-N(7) 2.128	N(7)-Ir(2)-N(8) 76.77
		Ir(2)-N(8) 2.133	
Average ^a	Ir-C 2.022	Ir-N(C [^] N) 2.063 Ir-N(N [^] N) 2.131	C-Ir-N 79.74 N-Ir-N 76.69

^aAverage data of bond lengths and angles of complex **1** from X-ray crystallography data.

Table S2. Bond lengths and angles of complex **1** from calculated results.

	Ir-C (Å)	Ir-N (Å)	Angles(°)
Complex 1	Ir-C 2.034	Ir-N(C [^] N) 2.096	C-Ir-N 79.88
		Ir-N(N [^] N) 2.202	N-Ir-N 75.12

Table S3. Contribution of iridium to selected HOMOs of complexes **1** and **2**.

Molecular orbital	Contribution of iridium (%)	
	Complex 1	Complex 2
H	21.28	34.41
H-1	0.83	14.86
H-2	-	10.67
H-4	-	6.02
H-5	-	8.03

Table S4. Device characteristics of red OLEDs based on complexes **1** and **2**.

Complex	Ratio [%]	V_{on}^{a} [V]	Max CE ^b [cd A ⁻¹]	CE ^b at 10 ³ cd m ⁻² [cd A ⁻¹]	CE ^b at 10 ⁴ cd m ⁻² [cd A ⁻¹]	Max EQE ^c [%]	Max PE ^d [lm W ⁻¹]	Max L^{e} [cd m ⁻²]	$\lambda_{\text{EL}}^{\text{f}}$ [nm]	CIE ^g (x, y)
1	0.8	2.6	8.2	7.2	1.6	6.0	7.1	10.3×10 ³	600,650(sh)	(0.63,0.37)
	1.0	2.7	9.2	8.1	-	6.7	7.7	9.7×10 ³	600,650(sh)	(0.63,0.37)
	1.2	2.7	9.8	8.6	-	7.2	8.1	10.0×10 ³	600,650(sh)	(0.63,0.37)
	1.4	2.7	9.7	8.7	-	7.1	8.2	9.5×10 ³	600,650(sh)	(0.63,0.37)
2	1.4	2.4	7.1	7.0	3.5	7.8	5.2	19.2×10 ³	628	(0.66,0.34)
	1.9	2.4	7.9	7.7	3.8	9.1	6.0	19.1×10 ³	634	(0.66,0.33)
	2.2	2.4	8.8	8.7	4.2	10.3	6.8	18.7×10 ³	632	(0.67,0.33)
	2.5	2.5	7.1	6.7	3.6	7.8	5.4	20.0×10 ³	628	(0.66,0.34)

^a V_{on} , turn-on voltage. ^bCE, current efficiency. ^cEQE, external quantum efficiency. ^dPE, power efficiency. ^e L , luminance. ^f λ_{EL} , EL wavelength, *sh* denotes the shoulder peak. ^gCIE, Commission Internationale de l'Éclairage.